Many-body calculation of the spatial extent of the wave function of a nonmagnetic impurity in a *d*-wave high-temperature superconductor using the *t-J* model

Manuela Capello[1] and Didier Poilblanc[2,1]
[1]*Laboratoire de Physique Théorique, CNRS and Université de Toulouse, F-31062 Toulouse, France*
[2]*Institute of Theoretical Physics, Ecole Polytechnique Fédérale de Lausanne, CH-1015 Lausanne, Switzerland*
(Received 12 March 2009; revised manuscript received 28 April 2009; published 8 June 2009)

Scanning tunneling microscopy (STM) by providing images of the effects of individual zinc impurities in cuprate superconductors with unprecedented atomic resolution offers a stringent test to models of correlated fermions for high-temperature superconductors. Using a *t-J* model supplemented by variational Monte Carlo many-body techniques, the spatial dependence of the hole density and of the valence bond and superconducting pairing amplitudes around the impurity are computed. Our calculation supplemented by the theory of interlayer tunneling by I. Martin *et al.* [Phys. Rev. Lett. **88**, 097003 (2002)] can explain most features of the STM experiments including the cross-shaped spatial structure and the impurity "resonant" peak.

DOI: 10.1103/PhysRevB.79.224507 PACS number(s): 74.20.Mn, 67.80.kb, 75.10.Jm

I. INTRODUCTION

Cuprates superconductors can be considered as doped two-dimensional (2D) Mott insulators where electronic correlations play a dominant role.[1,2] A number of exotic properties such as the pseudogap behavior reflect the complexity of the system. In a pioneering work, Anderson[3] proposed the resonating valence bond (RVB) Mott insulator as the relevant underlying *parent* state from which gapless *d*-wave superconductivity naturally emerges under doping. Within this scenario, the pseudogap naturally emerges as the energy scale associated with the formation of singlet electron pairs via the nearest-neighbor antiferromagnetic (AF) exchange. A mean-field version of the RVB theory using a *t-J* model[1] could also explain a number of bulk experimental observations.[4]

Local probes of correlated materials with atomic resolution have recently become possible thanks to scanning tunneling microscopy (STM) (Ref. 5) which provided unprecedented high-resolution maps of the surface of some underdoped cuprate superconductors.[6] The measured space-resolved doped-hole charge density in the superconducting (SC) regime of Na-CCOC and Dy-Bi2212 cuprates revealed stripe patterns.[7] This discovery naturally raises the question whether such inhomogeneities are induced by impurities or whether they are intrinsic as the bulk static charge and spin stripe orders detected in neutron-scattering experiments and recent resonance x-ray scattering in $La_{1.48}Nd_{0.4}Sr_{0.12}CuO_4$ (Ref. 8) and $La_{1.875}Ba_{0.125}CuO_4$ (Ref. 9) cuprates at doping $\delta \sim 1/8$.

Substituting a single impurity atom for a copper atom indeed strongly affects its surrounding region. Therefore, it can serve as a local fine probe, providing important insights into the properties of the correlated medium itself.[10,11] Imaging the effects of individual zinc impurity atoms on superconducting Bi2212 performed by STM (Ref. 12) showed clear real-space modulations and an impurity "resonance" peak which can be confronted to theoretical modeling. In other words, such observations offer a new stringent test to models of correlated fermions for high-temperature superconductors. It has been argued that a number of bulk properties of these materials can be explained within the correlated *t-J* model.[13] However, local real-space (charge) responses have been calculated at the mean-field level only.[14] Due to the short superconducting coherence length, a fully many-body approach is desirable.[15] Here, we have carried out such a program of (i) computing within a many-body numerical technique the response induced by the introduction of a spinless impurity site within a bulk two-dimensional *t-J* model and (ii) confronting the theoretical results to the experimental observations which might either invalidate the model or, on the contrary, bring additional credibility to it.

The $t-J$ Hamiltonian on a square lattice reads,

$$H_{t-J} = -\sum_{\langle i,j\rangle\sigma} t_{ij}(c^{\dagger}_{i\sigma}c_{j\sigma} + \text{H.c.}) + \sum_{\langle i,j\rangle} J_{ij}S_i \cdot S_j. \qquad (1)$$

A zinc impurity is in the same 2+ oxidation state as the copper ion it is substituted for, so that it does not introduce extra charge. However, in contrast to the copper $S=1/2$ ion, the Zn^{2+} ion is in a spin-singlet state, inert magnetically. Hence, one can use a simple description; on the four bonds connected to the impurity site we set $t_{ij}=0$ and $J_{ij}=0$ as shown in Fig. 1. Previous work[16] has shown that this description is not in contradiction to the observed spectral weight directly at the impurity site. On all the other bonds, we set t_{ij} and J_{ij} to the same values t and J, respectively. Although

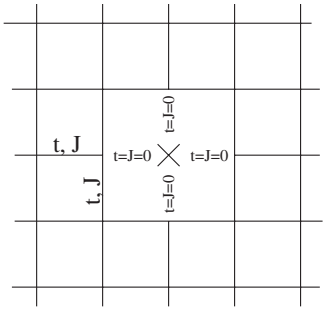

FIG. 1. Schematic representation of the impurity model. The cross corresponds to the impurity site i_0. The parameters t and J are set to zero on the four bonds connected to the impurity site.

completely local such a "boundary" is expected to lead to a *spatially extended* perturbation strongly affecting ground-state (GS) properties.

II. DESCRIPTION OF METHOD

Variational fully projected fermionic wave functions[17] (WF) are known to incorporate very satisfactorily correlation effects of the t-J model. We have extended them to finite periodic $L\times L$ clusters containing a single impurity (in practice $L=8$ and $L=16$). A variational Monte Carlo (VMC) scheme[17] is used to (i) realize a thorough optimization over the variational parameters[18,19] (see below) and (ii) to calculate the GS physical observables. The presence of the impurity on site i_0 modifies the Hilbert space, i.e., $c^\dagger_{i_0\sigma}|\Psi\rangle=0$ and $c_{i_0\sigma}|\Psi\rangle=0$, where $|\Psi\rangle$ is the GS of the system. In our Monte Carlo variational scheme an "impurity projector" $\mathcal{P}_{i_0}=(1-n_{i_0\uparrow})(1-n_{i_0\downarrow})$ is inserted, and the impurity variational wave function is defined as $|\Psi_{\mathrm{VMC}}\rangle=\mathcal{P}_g\mathcal{P}_{i_0}|D\rangle$, where $\mathcal{P}_g$ is the usual Gutzwiller projector enforcing the constraint of no-double occupancy on the remaining L^2-1 sites.

Motivated by the success of the RVB theory to explain bulk properties[4] the mean-field determinant $|D\rangle$ is chosen to be the ground state of a mean-field Hamiltonian of standard BCS-type,

$$H_{\mathrm{MF}}=\sum_{\langle i,j\rangle\sigma}(\chi_{ij}c^\dagger_{i\sigma}c_{j\sigma}+\mathrm{H.c.})+\sum_{\langle i,j\rangle}(\Delta_{ij}c^\dagger_{i\uparrow}c^\dagger_{j\downarrow}+\mathrm{H.c.})+\mu\sum_{i\sigma}n_{i\sigma},\tag{2}$$

defined on *all* of the $L\times L$ sites, including the i_0 site (always occupied by a hole). χ_{ij} and Δ_{ij} are variational parameters governing the bond hopping and bond singlet amplitudes. We optimize all different nonequivalent bonds around the impurity, starting from an initial guess, respecting or not the square lattice symmetry around i_0. Since in principle the Hamiltonian C_{4v} symmetry around i_0 (see Fig. 1) could be spontaneously broken, we have performed a number of preliminary tests on small 8×8 lattices choosing the initial RVB bonds pattern with lower symmetries such as, e.g., C_4 or C_{2v} symmetries (the latter allowing the formation of a domain wall). We have found that the full C_{4v} symmetry is systematically restored at the variational minimum. Therefore, to reduce the number of variational parameters and gain accuracy, the C_{4v} symmetry has been enforced on our largest 16×16 cluster. As expected, all optimized WFs are found to show opposite signs of Δ_{ij} on any site-sharing vertical and horizontal bonds, hence reflecting the expected *orbital* d-wave character of the superconducting order. Lastly, we note that allowing *finite* values of the parameters Δ_{ij} and χ_{ij} on the four bonds connected to the impurity is also important to gain energy as shown in Table I showing variational energies of Hamiltonian (1). The lowest-energy state (II) is obtained for a full optimization of the Δ_{ij} and χ_{ij} parameters over *all bonds*. Typically, χ_{ij} has a significant magnitude on the four bonds connected to the impurity site. Moreover, for decreasing doping, a sizable amplitude of Δ_{ij} also appears on the latter bonds. Note however that the *physical* bond amplitudes are still vanishing on the impurity bonds as expected.

TABLE I. Variational energy per site (in units of t) for different projected WFs for the t-J model at doping $1/8(N_h=8)$, for $t/J=3$, and a 8×8 cluster with an impurity. (I) $|D(8\times 8)\rangle$ is optimized fixing $\Delta_{ij}=0$, $\chi_{ij}=0$ around the impurity and $\mu_{i_0}=0$. Everywhere else Δ_{ij} is optimized and $\chi_{ij}=1$; (II) $|D(8\times 8)\rangle$ is fully optimized. The total energy difference between (I) and (II) is $\sim 0.3t$ per impurity.

$\lvert D\rangle$	(I)	(II)
$E_{\mathrm{VMC}}[t]$	−0.41493(5)	−0.41968(5)

III. RESULTS ON 16×16 CLUSTERS

We now turn to the VMC calculations on the 16×16 cluster with periodic-boundary conditions, assuming a physical value of $t/J=3$. Here we consider a physical "core" 8×8 region centered around the impurity (i.e., of the same size as our previous small cluster) where we impose a C_{4v} symmetry around the impurity site. Outside, we assume a uniform d-wave superconducting background (bg) whose parameters $\chi_{i,i+\hat{x}}=\chi_{i,i+\hat{y}}=\chi_{\mathrm{bg}}$ and $\Delta_{i,i+\hat{x}}=-\Delta_{i,i+\hat{y}}=\Delta_{\mathrm{bg}}$ are optimized simultaneously. This enables to reduce significantly the boundary effects and is justified since the spatial extension of the effect of the impurity rarely exceeds the assumed size of the core.

The spacial distribution of the local-hole density $\langle c_{i\sigma}c^\dagger_{i\sigma}\rangle$, the bond-hole kinetic amplitudes $K_{ij}=\langle(c_{j\sigma}c^\dagger_{i\sigma}+\mathrm{H.c.})\rangle$, and the magnetic VB amplitudes $S_{ij}=\langle\mathbf{S}_i\cdot\mathbf{S}_j\rangle$ are shown in Figs. 2(a) and 3(a), respectively, for doping 1/8. Here and throughout the paper, we only show the 6×6 central region exhibiting the largest modulations. It turns out that the variational parameters Δ_{ij} are suppressed on the four bonds connected to the impurity. This is compensated by an increase in Δ_{ij} and hence in S_{ij} on the neighboring bonds forming a crosslike structure [see thick blue bonds of Fig. 3(a)]. Due to similarities with work done in a somewhat different context,[21] we shall refer to these bonds as the four "dimer bonds". These bonds are characterized by a simultaneous hole deficiency and a large gain in the magnetic energy (which can reach more than 40%), hence signaling a tendency toward singlet crystallization around the impurity. The distribution of K_{ij} in Fig. 2 also shows a remarkably strong modulation around the impurity.

Superconducting properties of RVB states are characterized by the singlet-pair correlations at distance $\mathbf{r}$ $\langle\Psi_{\mathrm{VMC}}|\tilde{\Delta}^\dagger_{\mathbf{s}+\mathbf{r}}\tilde{\Delta}_{\mathbf{s}}|\Psi_{\mathrm{VMC}}\rangle/\langle\Psi_{\mathrm{VMC}}|\Psi_{\mathrm{VMC}}\rangle$, where the operator $\tilde{\Delta}^\dagger_{\mathbf{s}}=c^\dagger_{i(\mathbf{s}),\uparrow}c^\dagger_{j(\mathbf{s}+\hat{\mathbf{a}}),\downarrow}-c^\dagger_{i(\mathbf{s}),\downarrow}c^\dagger_{j(\mathbf{s}+\hat{\mathbf{a}}),\uparrow}$ creates a singlet pair of electrons on the bond between locations $\mathbf{s}$ and $\mathbf{s}+\hat{\mathbf{a}}$ on the lattice, $\hat{\mathbf{a}}$ being the unit vector that specifies the bond direction (along x or y). On the 8×8 cluster, the pairing correlations between separate bonds at the largest available distance do not completely reach saturation. To get a better estimation of the superconducting order parameter we have considered the 16×16 cluster and computed the pairing amplitudes $\bar{\Delta}_{ij}$ for all bonds (i,j) within the core region

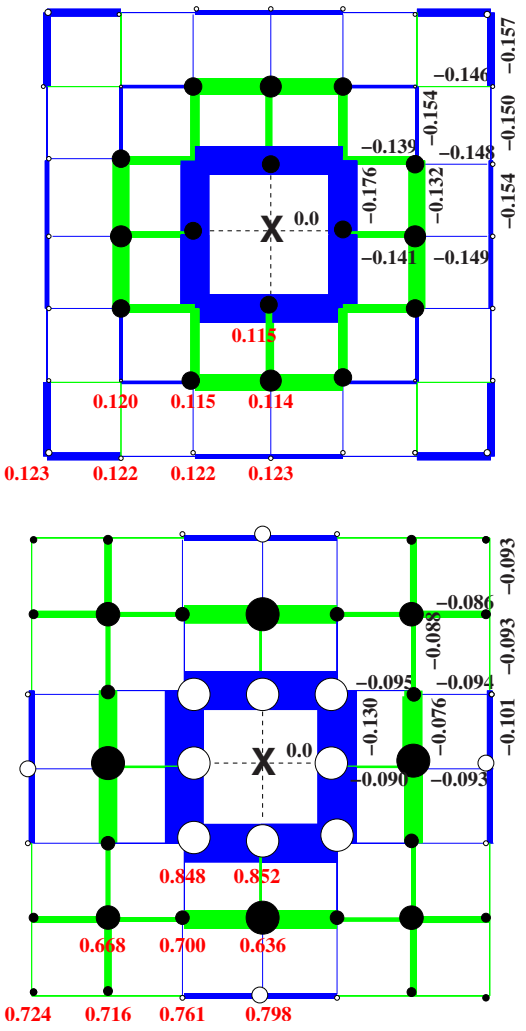

FIG. 2. (Color online) VMC results for the GS on-site hole densities (circles) and kinetic bond amplitudes K_{ij} (colored segments) obtained on a 16×16 cluster. Only the central region around the impurity is shown. Diameters of circles and widths of segments scale with the *absolute value* of the *relative* differences with respect to the impurity-free homogenous state estimated at the same δ_{ave} hole density (Ref. 20). Higher (lower) hole densities and bond magnitudes with respect to the homogeneous case are shown by open (filled) circles and blue (green) bonds respectively. For completeness, we also show on the plot the (bare) numerical values of the hole densities (in red) and bonds amplitudes (in black) (in (b) the hole densities have been multiplied by 10 for convenience). (a) and (b) corresponds to 32 ($\delta_{\text{ave}}\simeq0.1216$) and 20 ($\delta_{\text{ave}}\simeq0.0745$) doped holes giving rise, for an homogeneous background, to $E_{\text{kin}}^{\text{homog}}/t=-0.1487$ and $E_{\text{kin}}^{\text{homog}}/t=-0.0941$ per bond, respectively.

$$\bar{\Delta}_{i(\mathbf{s}),j(\mathbf{s}+\hat{\mathbf{a}})}=\frac{\langle\tilde{\Delta}_{\mathbf{s}}\tilde{\Delta}_{\text{bg}}\rangle}{\sqrt{\langle\tilde{\Delta}_{\text{bg}}\tilde{\Delta}_{\text{bg}}\rangle}},\tag{3}$$

where $\tilde{\Delta}_{\text{bg}}$ is a pair operator on the most remote bond in the homogeneous background. As shown in Fig. 4(a), pairing is enhanced on the dimer bonds and is depleted around the impurity, where holes are less present.

The 16×16 cluster also allows to reduce the doping content, e.g., to 20 holes, going further into the under-doped region. Interestingly, the hole distribution around the defect is very sensitive to the doping ratio. Indeed, for doping around 12.5% (32 holes) we found that holes are slightly repelled from the bonds around the impurity. In contrast, for 7.8% doping, holes tend to concentrate more around the impurity site as shown in Fig. 2(b). The variational pairing Δ_{ij} becomes stronger on the impurity bonds suggesting the formation of a "hole pair" with the impurity *empty* site. The corresponding real-space modulations of S_{ij} and $\bar{\Delta}_{ij}$ are shown in Figs. 3(b) and 4(b).

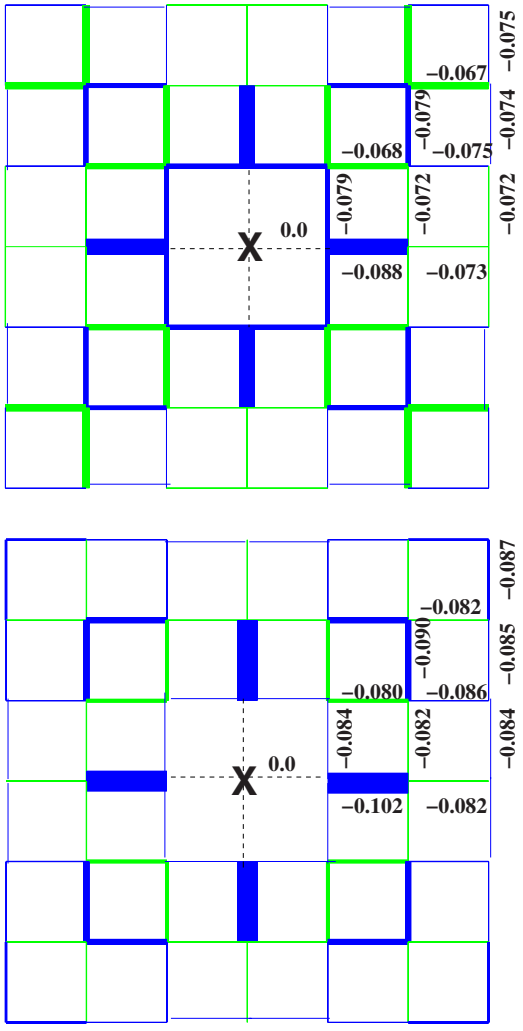

FIG. 3. (Color online) VMC results for the GS magnetic bond amplitudes S_{ij} obtained on a 16×16 cluster. Same conventions and parameters as in Fig. 2. (a) and (b) corresponds to 32 ($\delta_{\text{ave}}\simeq0.1216$) and 20 ($\delta_{\text{ave}}\simeq0.0745$) doped holes giving rise, for an homogeneous background, to $E_{\text{mag}}^{\text{homog}}/J=-0.074$ and $E_{\text{mag}}^{\text{homog}}/J=-0.084$ per bond, respectively.

IV. DISCUSSIONS

Let us now compare our findings to prior theoretical approaches. The first investigation of a single impurity immersed in a correlated host has been performed using Lanczos exact diagonalization of small clusters. A calculation of the local density of states[22] revealed bound states (of differ-

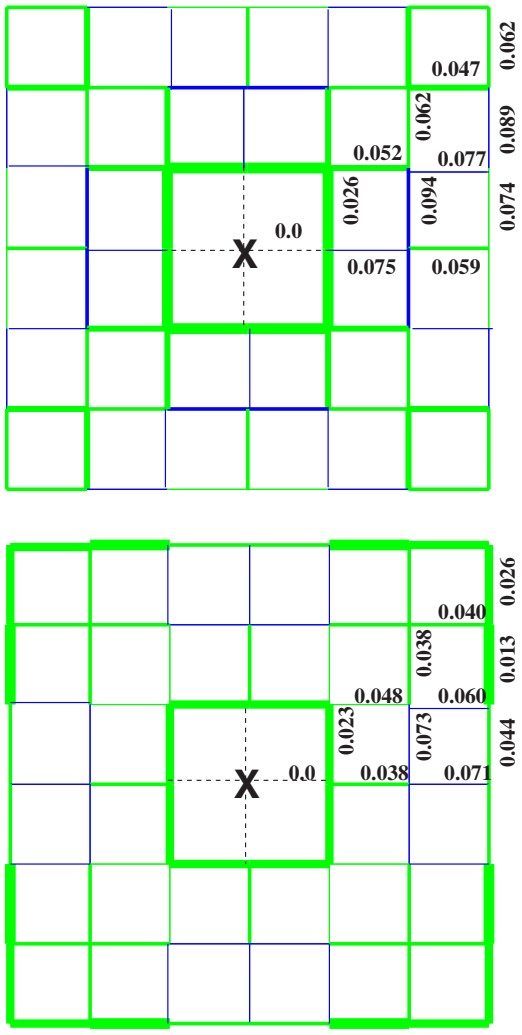

FIG. 4. (Color online) VMC results for the pairing bond amplitudes $\bar{\Delta}_{ij}$ obtained on a 16×16 cluster. Same conventions and parameters as in Fig. 2. (a) and (b) corresponds to 32 ($\delta_{\mathrm{ave}}\simeq0.1216$) and 20 ($\delta_{\mathrm{ave}}\simeq0.0745$) doped holes giving rise, for an homogeneous background, to $\Delta_{\mathrm{bg}}\simeq0.0787$ and $\Delta_{\mathrm{bg}}\simeq0.0626$, respectively.

ent orbital symmetries) in which a mobile hole is trapped by the induced impurity potential. Here, a unique mobile hole was assumed in the cluster, hence preventing real bulk pairing and giving rise to a very small doping $\sim5\%$ in the surrounding region. Although our VMC calculations are done in a different physical range (and on much larger clusters), we find, for decreasing doping, the emergence of excess hole density around the impurity, which possibly could be consistent with a bound-state formation when $\delta\rightarrow0$.

Metlitski and Sachdev[23] have introduced a theory of valence-bond solid (VBS) correlations near a single impurity in a square lattice antiferromagnet. When the system is close to a quantum transition from a magnetically ordered Néel state to a spin-gap state with long-range VBS order, a missing spin gives rise to a VBS pinwheel (or "vortex") around the impurity.[21] To compare with these predictions we have computed the VBS order parameter of Eq. (5) in Ref. 21. However, despite many similarities (e.g., crystallization of dimer bonds in the vicinity of the impurity), the vortex structure is not recognizable in our simulation. We hypothesize that (i) our system is probably not close enough to the critical point assumed in Refs. 21 and 23 and/or (ii) the VBS region develops differently in a *d*-wave RVB than in an AF background.

Lastly, our results are compared to the experimental STM observations around a Zn impurity in a Bi2212 cuprate superconductor shown in Ref. 12. First, we point out that GS properties have been calculated here while Ref. 12 reports spectral properties. However, since equal-time and frequency-dependent quantities are related via a simple frequency integration up to a physical cutoff (see, e.g., Ref. 7 for a derivation of the local hole-charge distribution from space-resolved tunneling spectra) both sets of data should reveal similarities. Indeed, like in the experiments, the patterns we found show clearly a cross-shaped symmetric structure. For a closer comparison, subtleties of the STM measurements in the cuprates have to be taken into account. First, we note that bond variables in our calculation could be directly compared to STM observations on top of the oxygen atoms of the Cu-O plane. Second, Martin *et al.*[16] have recently suggested that tunneling on top of a particular Cu or Zn atom in the Cu-O plane measures a linear combinations of its neighbors. Then, the enhanced density of states (a many-body effect due to the proximity of the Mott insulator) found in our calculations on the neighboring sites of the Zn impurity naturally explains the origin of the mysterious "resonant peak" found experimentally when the STM tip is located on the Zn atom. This finding provides a strong evidence that (i) the theoretical modeling of the impurity as an empty site and (ii) the use of the strongly correlated *t-J* model to describe the bulk high-T_c superconductor are realistic. Note also that the tendency of electrons to *avoid* the impurity obtained within a mean-field scheme (Gutzwiller approximation) (Ref. 14) is consistent with our findings but (i) with a quantitatively weaker amplitude and (ii) only *at low enough dopings*. In contrast, at intermediate doping $\sim12\%$ we find the opposite (weak) effect.

ACKNOWLEDGMENTS

We acknowledge support from the French Research Council (ANR). D.P. also thanks S. Sachdev and I. Zaanen for insightful discussions.

[1] F. C. Zhang and T. M. Rice, Phys. Rev. B **37**, 3759 (1988).
[2] S. Sachdev, Rev. Mod. Phys. **75**, 913 (2003).
[3] P. W. Anderson, Science **235**, 1196 (1987).
[4] F. C. Zhang, C. Gros, T. M. Rice, and H. Shiba, Supercond. Sci. Technol. **1**, 36 (1988).
[5] O. Fischer, M. Kugler, I. Maggio-Aprile, C. Berthod, and C. Renner, Rev. Mod. Phys. **79**, 353 (2007).
[6] T. Valla, A. V. Fedorov, Jinho Lee, J. C. Davis, and G. D. Gu, Science **314**, 1914 (2006).
[7] Y. Kohsaka *et al.*, Science **315**, 1380 (2007); J. Zaanen, Science **315**, 1372 (2007).
[8] J. M. Tranquada B. J. Sternlieb, J. D. Axe, Y. Nakamura, and S. Uchida, Nature (London) **375**, 561 (1995); N. B. Christensen, H. M. Ronnow, J. Mesot, R. A. Ewings, N. Momono, M. Oda, M. Ido, M. Enderle, D. F. McMorrow, and A. T. Boothroyd, Phys. Rev. Lett. **98**, 197003 (2007).
[9] P. Abbamonte, A. Rusydi, S. Smadici, G. D. Gu, G. A. Sawatzky, and D. L. Feng, Nat. Phys. **1**, 155 (2005); J. M. Tranquada G. D. Gu, M. Hücker, Q. Jie, H.-J. Kang, R. Klingeler, Q. Li, N. Tristan, J. S. Wen, G. Y. Xu, Z. J. Xu, J. Zhou, and M. v. Zimmermann, Phys. Rev. B **78**, 174529 (2008).
[10] M. I. Salkola, A. V. Balatsky, and D. J. Scalapino, Phys. Rev. Lett. **77**, 1841 (1996).
[11] For a recent review on experiments and theory of impurities in high-T_c cuprates see H. Alloul, J. Bobroff, M. Gabay, and P. J. Hirschfeld, Rev. Mod. Phys. **81**, 45 (2009).
[12] S. H. Pan, E. W. Hudson, K. M. Lang, H. Eisaki, S. Uchida, and J. C. Davis, Nature (London) **403**, 746 (2000).
[13] E. Dagotto, Rev. Mod. Phys. **66**, 763 (1994); M. Ogata and H. Fukuyama, Rep. Prog. Phys. **71**, 036501 (2008),and references therein.
[14] H. Tsuchiura, Y. Tanaka, M. Ogata, and S. Kashiwaya, Phys. Rev. B **64**, 140501(R) (2001).
[15] The magnetic response induced by a single impurity has been computed within a similar VMC scheme. See Shi-Dong Liang and T. K. Lee, Phys. Rev. B **65**, 214529 (2002).
[16] I. Martin, A. V. Balatsky, and J. Zaanen, Phys. Rev. Lett. **88**, 097003 (2002).
[17] C. Gros, Phys. Rev. B **38**, 931 (1988); S. Sorella, G. B. Martins, F. Becca, C. Gazza, L. Capriotti, A. Parola, and E. Dagotto, Phys. Rev. Lett. **88**, 117002 (2002).
[18] For other VMC studies of nonuniform correlated states see M. Capello, M. Raczkowski, and D. Poilblanc, Phys. Rev. B **77**, 224502 (2008).
[19] Strictly speaking, the surrounding medium has N_h-1 mobile holes, i.e., an average doping $\delta_{\text{ave}}=(N_h-1)/(L^2-1)$ lower than the nominal doping $\delta=N_h/L^2$.
[20] The related values for the impurity-free homogenous state are estimated at the same δ_{ave} hole density by a simple linear interpolation between pure clusters with the available flanking hole densities.
[21] R. K. Kaul, R. G. Melko, M. A. Metlitski, and S. Sachdev, Phys. Rev. Lett. **101**, 187206 (2008); M. A. Metlitski and S. Sachdev, Phys. Rev. B **78**, 174410 (2008).
[22] D. Poilblanc, D. J. Scalapino, and W. Hanke, Phys. Rev. Lett. **72**, 884 (1994).
[23] M. A. Metlitski and S. Sachdev, Phys. Rev. B **77**, 054411 (2008).